

## THE EFFECT OF WATER'S PRESENCE AROUND THE PHASE CHANGE MATERIAL

by

**Haythem SHILI<sup>a,c,\*</sup>, Kamel FAHEM<sup>a</sup>, Souad HARMAND<sup>b</sup>,  
and Sadok BEN JABRALLAH<sup>a,c</sup>**

<sup>a</sup> Laboratory of Energetics and Thermal and Mass Transfer (LETTM), Faculty of Sciences of Tunis,  
University of Tunis El Manar, Campus Universitaire, Tunisia

<sup>b</sup> University Lille Nord de France, Lille, Valenciennes, France

<sup>c</sup> Faculty of Science of Bizerte, University of Carthage, Bizerte, Tunisia

Original scientific paper

<https://doi.org/10.2298/TSC180922301S>

*As part of the research in the field of thermal control of electronic components, a phase change material is confined in a liquid and is heated vertically on one side by a hot plate. The presence of the liquid around the phase change material prevents the formation of air bubbles produced in case of direct contact between the hotplate and the phase change material (extends the lifetime of the phase change material by reducing overheating zones). It improves heat transfer by increasing the thermal conductivity around the phase change material (raising the thermal exchange surface) and by accelerating the convective transfer. This work examines experimentally and numerically the effect of the water on the phase change material and on the heating plate. The water is used around the phase change material and a comparative study of the comportment of some important parameters like the melt front form, melting time, flow direction, temperature, and operating time is realized. It is found that the presences of the liquid around the phase change material seems to be more interesting for a thermal protection role than the standard case of the phase change material directly heated by the hotplate.*

*Key words: experimental set-up, numerical model, phase change materials, melting, heat transfer, cooling electronics*

### Introduction

The presence of a thermal protection system inside electronic devices helps in improving the performance as well as increasing the system's lifetime [1]. Without appropriate thermal management, the generation of heat and the warm-up can lead to the deterioration of electronic components. The conventional cooling methods, such as cooling by spraying (Jet spray [2], air spray [3]) or by forced convection [4], are no longer considered as appropriate techniques to use given the complexity of new systems and the aim to reduce energy consumption as well as the lack of physical spaces, especially for portable devices. Based on these considerations, the use of phase change materials (PCM) seems to be the most effective solution due to their high latent and specific heat, the presence of a controllable melting point and a small variation of volume during the phase change. The PCM can absorb a large amount of heat during the melting phase, which is a significant factor in energy dissipation from electronic

\* Corresponding author, e-mail: shilihaythem@gmail.com

components [5]. The PCM then have a far better heat dissipation compared to that evacuated using the conventional cooling methods. Several experimental and numerical studies have been conducted to promote the utility of PCM in the thermal protection field. Tan *et al.* [6] have shown experimentally that the use of *n*-eicosane helps to stabilize the temperature, whereas when we remove the PCM the temperature increases rapidly, and that the efficiency of the system depends on the quantity of PCM used. Kadri *et al.* [7] used an experimental set-up to study the dynamics of the melting process of a PCM in a rectangular enclosure for various temperatures on the hot boundary and several Fourier numbers. Gharbi *et al.* [8] presented an experimental study of PCM-based heat sinks for continuous and intermittent regimes for discrete heat sources. They noted that the best efficient arrangement of a higher power component is at the lower location and that dividing heat flux equally between middle and lower source seems suitable for applications with long operating time.

Another possibility to improve the phase change performance of a cooling system consists of finding solutions to enhance the conductivity. One of these solutions is the use of fins. Ashraf *et al.* [9] presented an experimental investigation focused on optimizing the passive cooling system using two geometries of pin-fin, six paraffin waxes and varying power levels, they noted that the circular inline is the most efficient choice for a PCM-based heat sink. Kandasamy *et al.* [10] showed that the inclusion of PCM in the cavities of the heat sinks increases the cooling performance. Rudonja *et al.* [11] noted that the insertion of rectangular copper fins along with the heating cylinder enhances the heat transfer and they could detect it thanks to the introduction of a geometric parameter named surface ratio. Huang *et al.* [12, 13] developed numerically two models: PV/PCM with and without fins, which they validated experimentally. They noticed that the presence of the metallic fins improves significantly the thermal performances of the system. On the other hand, they warned that the use of a larger number of fins could limit the movement of the melted PCM. Yang *et al.* [14] conducted an experimental study on a finned heat pipe integrated with a PCM heat sink. They analyzed different thermal shocks and presented a comparison between low melting point metal and an organic PCM. They reported that the PCM has great potentials for electronic thermal management applications and using the low melting point metal as PCM showed a prolonged working duration of 1.2-2.4 times compared to the conventional PCM. Salimpour *et al.* [15] noted that inserting metal fins is a brilliant technique for increasing the performance of PCM-based heat sinks and increasing its thickness influences the optimal number of fins inside the enclosure. Srikanth *et al.* [16] made an experimental investigation on the thermal performance of PCM-based cuboidal heat sinks with 72 pin-fins with four identical discrete heaters at the base. They reported that the discrete non-uniform heating has a significant effect on the thermal performance of the heat sink and that during the melting the ratio of the latent heat time to the sensible heating time remains the same for all the discrete heating cases.

Other researchers chose to use a porous matrix or to modify the material proprieties of PCM with nanoadditives to improve the thermal transfer inside it. Gharbi *et al.* [17] conducted a study on a model for thermal control of PCM-based heat sinks with some different configurations. They also observed that the presence of a graphite matrix provides better thermal control and that the use of the fins contributes to the melting process. Alshaer *et al.* [18] made an experimental study of a hybrid composite system for thermal management of electronic devices. They tested three models (carbon foam; carbon foam + paraffin; carbon + paraffin + nanocomposite). The analysis indicates that the addition of a nanocomposite appears to be more effective for carbon foam of relatively lower thermal conductivity. Li *et al.* [19] experimentally analyzed the thermal performance of the microencapsulated PCM/copper foam composite. It

was found that the addition of metal foam had improved the heat transfer and reduced the time consumption to start phase change. Zheng *et al.* [20] conducted an experimental and numerical study on a PCM embedded in a copper foam inside a rectangular enclosure under constant heat flux condition. They noticed that the melting time of composite PCM/copper foam was 20% shorter than the pure PCM and the temperature distribution became more uniform in PCM/copper foam composites.

When a PCM is encapsulated in containers, some space must be left to cope with the volume expansion of the PCM. A part of this air volume located at the top of the cell can infiltrate between the hot plate and the PCM and thus forms a contact resistance that slows down the heat transfer. This situation degrades the performances of the cell, slows down the heat transfer and reduces the lifetime of the PCM. This phenomenon is more visible by using plates with fins. Huang *et al.* [21] noticed that the use of horizontal fins increases heat transfer resistance by blocking the movement of bubbles formed by the fins during PCM melting. Moreover, Vasu *et al.* [22] reported that molten PCM such as  $\text{NaNO}_3$  corroded the foam structure and caused a chemical instability issue in the high temperature thermal storage system. To solve this problem and to improve the convective transfer in an electronic device's cooling system, confining the PCM in an enclosure filled with liquid is suggested.

### Experimental set-up

Experimental set-up, fig. 1, is constituted by a rectangular cell and a PCM surrounded by a liquid heated only by one of the vertical walls. The heating plate is provided by a resistance supplied by a current generator. The heating flux is controlled by acting on the current intensity. A digital camera was used to display the melting front evolution. The *K*-type thermocouples were also used to draw the profile of the temperature.

A schematic diagram of the apparatus employed in this investigation is shown in fig. 2. The experimental apparatus consists of two rectangular Plexiglas enclosures, the first one with inner dimensions of 75 mm (length), 25 mm (width), and 25 mm (depth), while the second one has inner dimensions of 80 mm (length), 30 mm (width), and 30 mm (depth). The idea is to fill the first one with the PCM and to confine it in the second one (filled with liquid) so that the liquid surrounds it.

The small enclosure is inserted in the middle of the large enclosure to have the same liquid film thickness for the four sides around the PCM (2.5 mm). A small smokestack is designed in order to leave an air gap to account for the PCM expansion that accompanies the solid-liquid phase change. The system is heated vertically on the right side by an electric resistance attached below stainless steel plate (inox

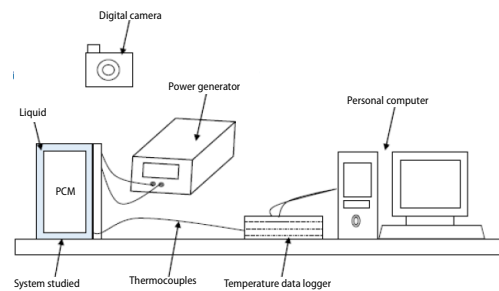


Figure 1. Experimental set-up

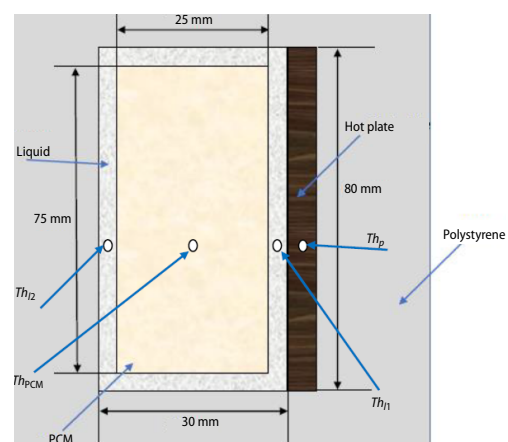


Figure 2. Schematic representation

304), tab. 1, with the inner dimensions of 80 mm (length), 10 mm (width), and 30 mm (depth) and joined to a power supply (Copley Controls Corp DSAO 1C).

**Table 1. Thermophysical properties of inox 304 [23]**

Materials	Density $\rho$ [kgm <sup>-3</sup> ]	Specific heat capacity $C_p$ [kJkg <sup>-1</sup> K <sup>-1</sup> ]	Thermal conductivity $\lambda$ [Wm <sup>-1</sup> K <sup>-1</sup> ]
Inox 304	7900	500	15

The walls of the system are made with transparent Plexiglas (2 mm thickness) to allow the photographic observation of the melting process and to minimize the heat loss from the enclosure by its low thermal conductivity. For further insulation, the system was insulated by polystyrene plates. The PCM used in this study was a commercial product, Plastic paraffin. Thermal properties of the PCM are reported below in tab. 2.

**Table 2. The PCM thermophysical properties [14]**

Materials	Latent heat $L_m$ [kJkg <sup>-1</sup> ]	Melting temperature $T_m$ [°C]	Density $\rho$ [kgm <sup>-3</sup> ]	Specific heat capacity $C_p$ [kJkg <sup>-1</sup> K <sup>-1</sup> ]	Thermal conductivity $\lambda$ [Wm <sup>-1</sup> K <sup>-1</sup> ]	Thermal expansion $\beta$ [K <sup>-1</sup> ]
Plastic paraffin	138.23	51.75	900(s)	2.710(s) (25 °C)	0.234(s)	10–5
			770(l)	4.640(s) (65 °C)	0.164(l)	

Four thermocouples with a calibrated accuracy of  $\pm 1$  °C have been placed inside the system to measure the transient temperature distribution. They were placed on the same horizontal line ( $x = 35$  mm), one on the hotplate, one in the film of the liquid near the plate, one in the PCM and finally one in the liquid film to the left of the PCM. All thermocouples were connected to the computer through a data logger (KEITHLEY 3706) to record temperature.

### Mathematical model

This study is assumed to be 2-D. The PCM is supposed to be pure, homogenous and with isotropic physical properties. The liquid PCM is considered, incompressible, Newtonian, and subjected to the Boussinesq approximation. Solid PCM particles are motionless inside the melted domain. Evaporation and condensation of water, tab. 3, are neglected (the enclosure

**Table 3. Thermophysical properties of water**

Materials	Density $\rho$ [kgm <sup>-3</sup> ]	Specific heat capacity $C_p$ [kJkg <sup>-1</sup> K <sup>-1</sup> ]	Thermal conductivity $\lambda$ [Wm <sup>-1</sup> K <sup>-1</sup> ]	Dynamic viscosity $\mu$ [Pas <sup>-1</sup> ]
Water	998.3	4185	0.6	$10^{-3}$

is totally filled by water and PCM capsule) and there is no contact between the water and the PCM. Based on the above assumptions and the enthalpy porosity model [24] the governing equations used here for the PCM are:

– Momentum equations:

$$\rho_l \left( \frac{\partial u}{\partial t} + u \frac{\partial u}{\partial x} + v \frac{\partial u}{\partial y} \right) = -\frac{\partial p}{\partial x} + \mu_l \left( \frac{\partial^2 u}{\partial x^2} + \frac{\partial^2 u}{\partial y^2} \right) + Bu \quad (1)$$

$$\rho_l \left( \frac{\partial v}{\partial t} + u \frac{\partial v}{\partial x} + v \frac{\partial v}{\partial y} \right) = -\frac{\partial p}{\partial y} + \mu_l \left( \frac{\partial^2 v}{\partial x^2} + \frac{\partial^2 v}{\partial y^2} \right) + \rho_0 g (T - T_0) + Bv \quad (2)$$

– Energy equation:

$$C_{p,\text{eq}} \left( \frac{\partial T}{\partial t} + u \frac{\partial T}{\partial x} + v \frac{\partial T}{\partial y} \right) = \lambda_{\text{eq}} \left( \frac{\partial^2 T}{\partial x^2} + \frac{\partial^2 T}{\partial y^2} \right) \quad (3)$$

The  $H$  is the liquid fraction, which is defined by the following relations:

$$\begin{cases} H = 0 & \text{if } T < T_m \\ H = 1 & \text{if } T > T_m \end{cases}, \quad T_m : \text{melting temperature} \quad (4)$$

During the process of the momentum equations resolution, the source term,  $B$ , serves to avoid the velocities fields in the solid region [24]:

$$B = C \frac{1 - H^2}{H^3 + b} \quad (5)$$

For this,  $C$  must be high enough, and  $b$  is a small number introduced here simply to avoid a division by zero in the case of  $H = 0$ .

The density and dynamic viscosity of the liquid PCM depend on its temperature. The density can be expressed as [10]:

$$\rho = \rho_0 g \beta (T - T_0) \quad (6)$$

where  $\beta$  is the thermal expansion.

The dynamic viscosity of the liquid PCM can be expressed:

$$\mu = 0.001 \exp \left( A + \frac{B}{T} \right) \quad (7)$$

where  $A = -4.25$  and  $B = 1760$  [10].

In the energy equation, both terms  $C_{p,\text{eq}}$  and  $\lambda_{\text{eq}}$  represent, respectively, the equivalent heat capacity and equivalent thermal conductivity:

$$C_{p,\text{eq}} = H(C_p)_l + (1 - H)(C_p)_s \quad (8)$$

$$\lambda_{\text{eq}} = H\lambda_l + (1 - H)\lambda_s \quad (9)$$

The initial and boundary conditions for  $u$ ,  $v$ , and  $T$  are shown in the fig. 3.

The numerical solution was carried out using COMSOL MULTIPHYSICS commercial software. This software was used to create and mesh the geometrical model and solve the governing equations previously described [25, 26]. This code uses discretization and a formulation based on the finite element method using quadratic Lagrangian elements. The direct solver UMFPAK was used as linear solver with a convergence of  $10^{-4}$ . The advantage of this solution sequence over a simultaneous solution to the transient momentum and energy equations is to prevent numerical convergence difficulties and to reduce numerical cost.

## Validation

### Grid independency

To solve this equation system, a meshing model was created, simple linear free triangular elements are used to create the overall mesh. A mesh independence study was performed

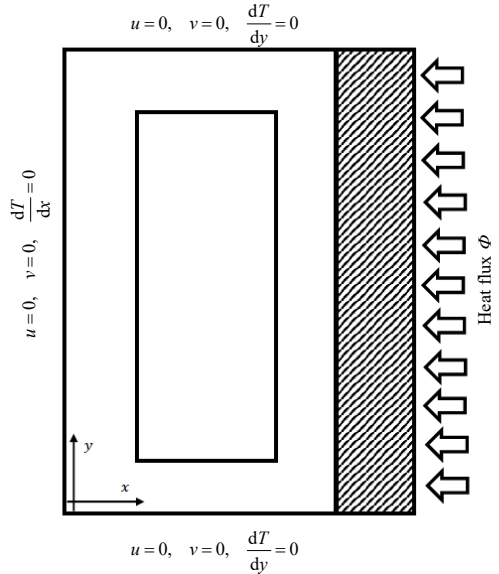


Figure 3. Initial conditions

Table 4. Mesh-independent

Number of elements	7514	11164	22720	34056
$H$	0.60	0.59	0.60	0.60
$T_p$ [°C]	80.83	80.79	80.85	80.85

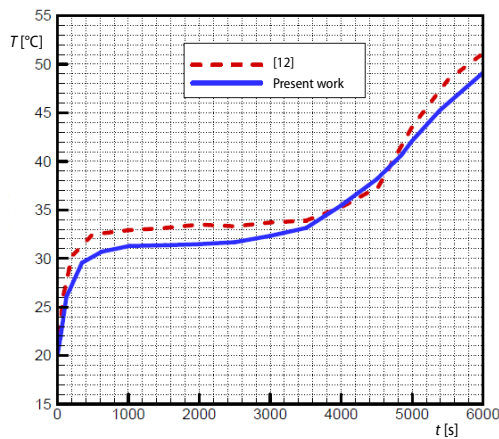


Figure 4. Variation of average copper plate temperature versus the time

**Result and discussion**

*Evolution of phase change interface*

The presence of the liquid is intended to prevent direct contact between the PCM and the hot plate and to enhance the active surface of the PCM cell. It also allows to improve

in order to determine the appropriate size of elements to be used and to provide an accurate mesh independent solution in order to limit the overall computation time. Four meshes were considered, 7514, 11164, 22720, and 34056 elements.

Table.4 reports the results of a grid independence test carried out on the evolution of PCM liquid fraction and the plate average temperature for the same instant  $t = 9000$  seconds. It can be observed that identical results are achieved with 22720 elements and 34066 elements. Therefore, a triangular mesh of 34056 elements was considered for this work.

*The PCM not surrounded by water*

The main objective of this work is the thermal protection of the electronic components, in order to see the interest using the liquid around the PCM, a numerical study of the case of PCM without liquid surrounding it was made.

Validations of the present mathematical model have been carried out by comparing code prediction of the plate average temperature with previous works. Figure 4 shows the comparison of code predictions with the work of Huang *et al.* [12]. As shown in the figure, the model present similar profiles and there is a close agreement.

*The PCM surrounded by water*

The results of the experiment were compared with the simulation to verify the numerical models developed for the case of the PCM surrounded by water. As can be seen, tab. 5 shows how the simulations fit the experimental results.

**Table 5. Experimental and numerical results**

Nature of study	Time of total melt $t$ [minute]	$Th_p$ [°C]	$Th_{l1}$ [°C]	$Th_{l2}$ [°C]	$Th_{PCM}$ [°C]
Experimental	212	83	65	63	61
Numerical	206	79.91	67.25	65.61	58.51
The difference	2.8 %	3.7 %	3.4 %	4.1 %	4 %

the conductivity in close proximity of the hotplate and improves the heat transfer because the convective transfer starts very quickly without waiting for the beginning of the PCM melting.

In the standard case where the PCM is indirect contact with a hot plate heated vertically from the external face, fig. 5, it is noticed that at the beginning the melting occurs in parallel to the heating plate (adjacent to the hot wall). The heat transfer mechanism is dominated by conduction. This mode continues as long as the viscous force is opposed to the fluid motion during which the solid-liquid interface remains almost uniform and parallel to the hot wall. As time progress, the buoyancy force becomes rather large and exceeds the viscous force (under the influence of the increase of the liquid zone) and the melting focuses on the high part of the cavity. The development of buoyancy force results in the formation of a growing circulating current in the top part of the enclosure creating a concave curvature at the top of the melting front (the natural convection). The inclination of the liquid-solid interface increases until the total fusion is reached.

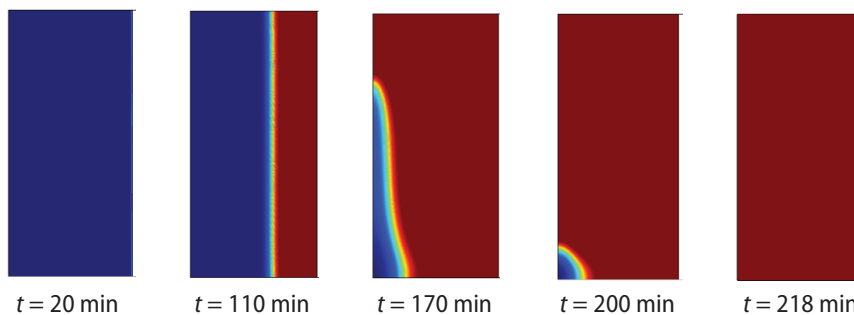


**Figure 5. Evolution of the melting front for PCM in direct contact with the hotplate**  
 (for color image see journal web site)

Figure 6 shows that the presence of the liquid around the PCM changed the form of the melting front. Thanks to the thermophysical properties of the liquid, the melting no longer happens on only one side (the side that is adjacent to the heated wall) and there has been an increase in the exchange surface. Under the convective effect, a circulation current is formed inside the water, which caused the distribution of the heat around the cavity of the PCM.

The increase of the exchange surface has for consequence an evolution of the melting front that is different from the standard case for a PCM in direct contact with a heating plate. At the beginning, the melting falls behind until the liquid warms up and reaches the temperature required for the phase change ( $T_m = 51.75^\circ$ ). When the liquid reaches this temperature, it is noticed that the melting begins on three sides (both vertical walls and the one at the top of the cavity). At the beginning and under the influence of the pure conduction, the PCM melts following a line parallel to every wall, then under the effect of natural convection, the melting becomes clearer and takes a concave form at the top of the PCM block. The melting is more accentuated on the top side and the neighboring side of the hotplate; this is due to thermal stratification effect.

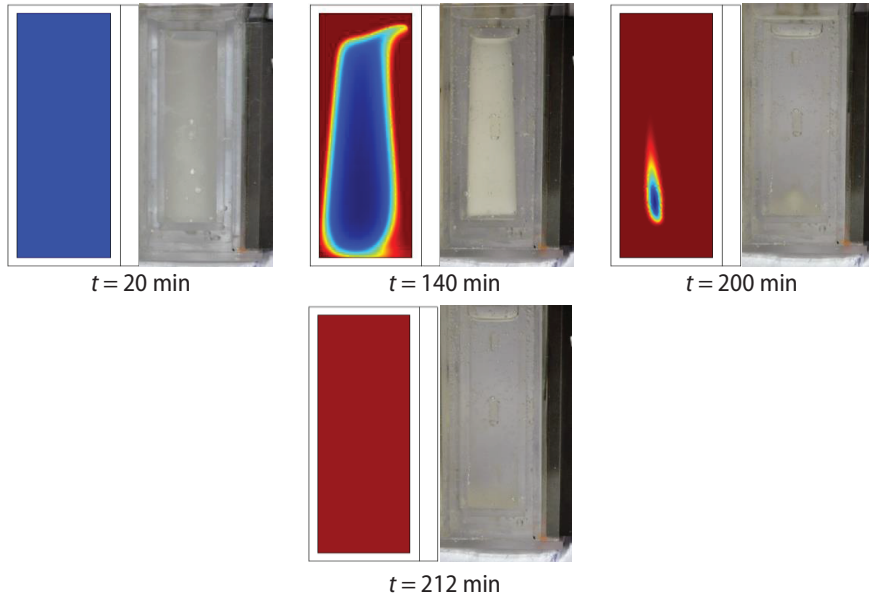


**Figure 6.** Comparison of the melting front between numerical (left) and experimental (right) results for the PCM surrounded by water  
(for color image see journal web site)

#### Velocity field vector

Figures 7 and 8 show the velocity field vectors induced by the natural convection in the liquid PCM (in blue arrows) and in the water surrounding the PCM (in red arrows) for four different percentages of melting. For the standard case, fig. 7, the evolution of the solid-liquid interface comes along with a laminar convective circulation in the liquid zone. The sense of velocity field vector follows the melt front.

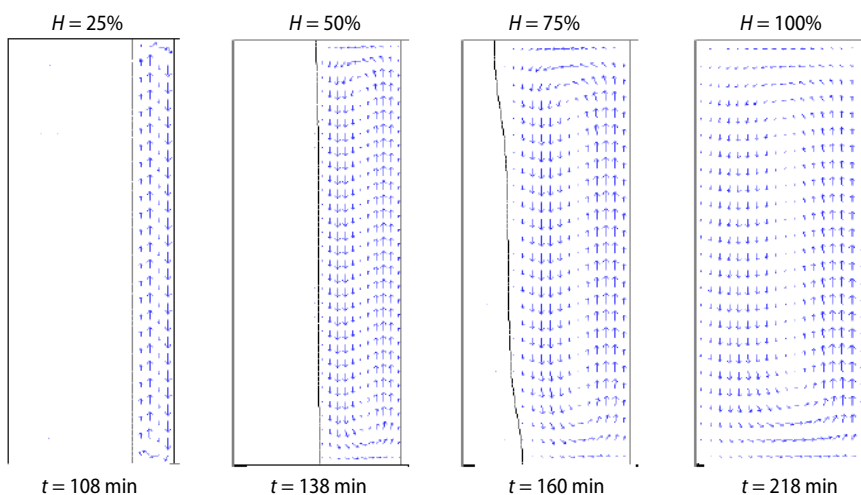


**Figure 7.** Velocity field vectors for PCM in direct contact with the hotplate  
(for color image see journal web site)

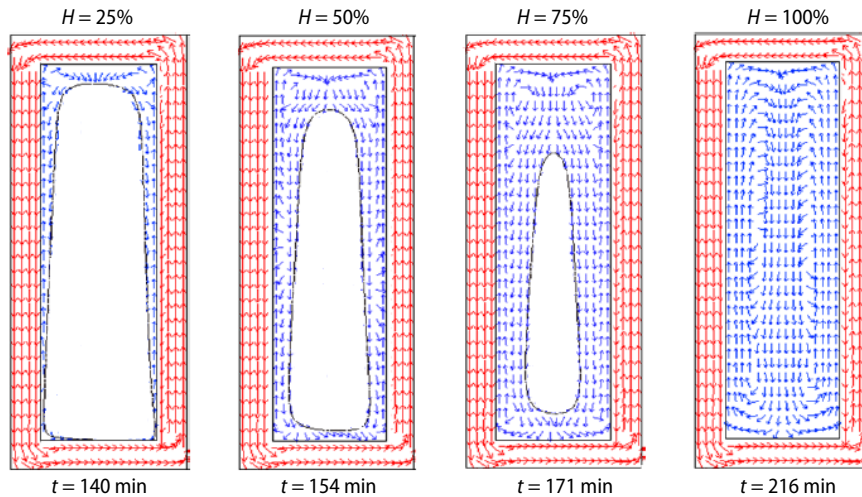


**Figure 8. Velocity field vectors for PCM surrounded by water**  
(for color image see journal web site)

As seen in fig. 8 the formation of a vortex around the PCM is noticed, it is explained by the buoyancy phenomenon where the hottest particles are pushed vertically and are directed from bottom to top and the cold particles take the opposite direction. The presence of a secondary vortex in contact with the PCM is also observed.

Inside the PCM, and due to the buoyancy effect (liquid zone), two smaller vortices formed near the top of the container that were growing following the melting process.

In order to clarify the direction of the velocity field vectors, fig. 8, it is important to remember that the same size for the arrows is used and that the velocity field in the liquid is larger than that of the melted part of the PCM.

### *Thermal behavior*

The presence of liquid improves heat transfer and prevents the direct contact between the PCM and the hot plate. It is observed, fig. 9, that when the total melting is reached, the presence of water decreases the temperature by, the liquid and PCM combination decreases the temperature of the hot plate compared to the case where only the PCM is used.

### *Operating time*

Keeping the heat source under a critical temperature for a long time represents a crucial challenge for several industrial applications. A comparative study of the operating time (it is the time taken by the component before reaching the critical temperature) was done. As can be seen in fig. 10, the presence of liquid around the PCM improves the operating time. The PCM and water association prolongs the operating time by compared to the case where only the PCM is used. This combination gives an improvement.

### **Conclusion**

An experimental and numerical study has been presented to determine the influence of the water's presence around the PCM. As compared to a standard case of a rectangular enclosure filled with a PCM and heated on a vertical wall, it is noticed that confining the PCM in the water are as follows.

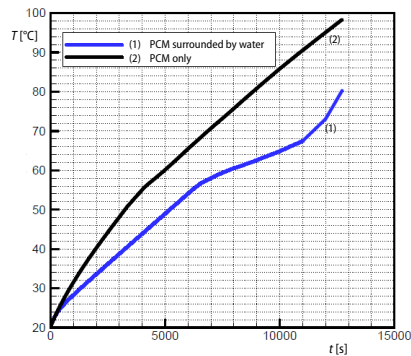


Figure 9. Variation of the temperature of the hotplate

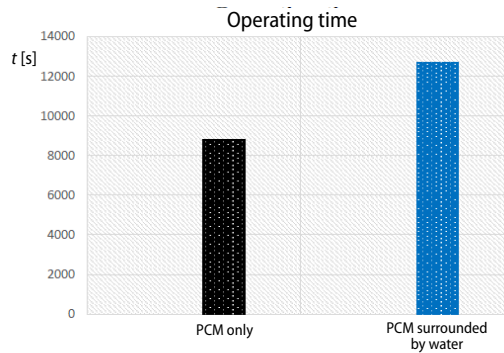


Figure 10. Comparison of the operating time

- Prevents any direct contact between the PCM and the hotplate, therefore, reduces the risks of having overheating zones (increases the life duration of the PCM).
- Enhances the thermal conductivity in close proximity of the hotplate.
- Reduces the quantity of the needed PCM.
- Improves the heat transfer and allows a better distribution of the heat (the melting occurs on the entire perimeter and not only on the part which is in direct contact with the hot plate).
- Decreases the temperature of the copper plate by almost 20%.
- Increases the operating time by 44%.

To improve the efficiency of this new design, future work could explore as follows.

- The opportunity to using other liquids then water.
- The opportunity to enhance the conductivity inside the liquid.
- Higher critical temperature to simulate other applications.

### Nomenclature

$A$	– constant
$B$	– source term
$b$	– constant
$C$	– constant
$C_p$	– specific heat, [ $\text{Jkg}^{-1}\text{K}^{-1}$ ]
$g$	– gravitational acceleration, [ $\text{ms}^{-2}$ ]
$H$	– liquid fraction.
$L_m$	– latent heat, [ $\text{Jkg}^{-1}$ ]
$t$	– time, [s]
$T$	– temperature, [K]
$Th$	– thermocouples
$u, v$	– velocity, [ $\text{ms}^{-1}$ ]
$x, y$	– co-ordinates, [m]

### Greek Symbols

$\beta$	– thermal expansion coefficient, [ $\text{K}^{-1}$ ]
$\phi$	– heat flux, [ $\text{Wm}^{-2}$ ]
$\lambda$	– thermal conductivity, [ $\text{Wm}^{-1}\text{K}^{-1}$ ]
$\rho$	– density, [ $\text{kgm}^{-3}$ ]
$\mu$	– dynamic viscosity, [Pas]

### Subscripts

0	– initial state
c	– critical
eq	– equivalent
l	– liquid
m	– melting
p	– hot plate
s	– solid

### References

- [1] Tilley, A. R., H. D. Associates, *The Measure of Man and Women, Human Factors in Design, Revised Edition, Whitney Library of Design*, Watson-Guptill Publications, New York, USA, 2001
- [2] Ebrahimiyan, V., *et al.*, Two-Dimensional Modeling of Water Spray Cooling in Superheated Steam, *Thermal Science*, 12 (2008), 2, pp. 79-88
- [3] Qiu, S., *et al.*, Enhanced Heat Transfer Characteristics of Conjugated Air Jet Impingement on a Finned Heat Sink, *Thermal Science*, 21 (2015), 1A, pp. 279-288

- [4] Bhattacharya, A., et al., Finned Metal Foam Heat Sinks for Electronics Cooling in Forced Convection, *J. Elect. Package*, 124 (2002), 3, pp. 155-163
- [5] Tso, C. P., et al., Transient and Cyclic Effects on a PCM-Cooled Mobile Device, *Thermal Science*, 19 (2015), 5, pp. 1723-1731
- [6] Tan, F.L., et al., Cooling of Mobile Electronic Devices Using Phase Change Materials, *Applied Thermal Engineering*, 24 (2004), 2-3, pp. 159-169
- [7] Kadri, S., et al., Large-Scale Experimental Study of a Phase Change Material: Shape Identification for the Solid-Liquid Interface, *Int. J. Thermophys*, 36 (2015), 10, pp. 2897-2915
- [8] Gharbi, S., et al., Experimental Study of the Cooling Performance of Phase Change Material with Discrete Heat Sources – Continuous and Intermittent Regimes, *Appl. Therm. Eng.*, 111 (2017), Jan., pp. 103-111
- [9] Ashraf, M. J., et al., Experimental Passive Electronics Cooling: Parametric Investigation of Pin-Fin Geometries and Efficient Phase Change Materials, *International J. of Heat and Mass Transfer*, 115 (B) (2017), Part B, pp. 251-263
- [10] Kandasamy, R., et al., Transient Cooling of Electronics Using Phase Change Material (PCM)-Based Heat Sinks, *Appl. Thermal Eng.*, 28 (2008), 8-9, pp.1 047-1057
- [11] Rudonja, N. R., et al., Heat Transfer Enhancement through PCM Thermal Storage by Use of Copper Fins, *Thermal Science*, 20 (2016), Suppl. 1, S251-S259
- [12] Huang, M. J., et al., Thermal Regulation of Building-Integrated Photovoltaics Using Phase Change Materials, *International Journal of Heat and Mass Transfer*, 47 (2004), 12-13, pp. 2715-2733
- [13] Huang, M. J., et al., Comparison of a Small-Scale 3D PCM Thermal Control Model with a Validated 2D PCM Thermal Control Model, *Solar Energy Materials & Solar Cells*, 90 (2006), 13, pp. 1961-1972
- [14] Yang, X. H., et al., Finned Heat Pipe Assisted Low Melting Point Metal PCM Heat Sink Against Extremely High Power Thermal Shock, *Energy Convers Manage*, 160 (2018), Mar., pp. 467-476
- [15] Salimpour, M. R., et al., Constructal Multi-Scale Structure of PCM Based Heat Sinks, *Continuum Mechanics and Thermodynamics*, 29 (2017), Nov., pp. 477-491
- [16] Srikanth, R., Experimental Investigation on the Heat Transfer Performance of a PCM Based Pin Fin Heat Sink With Discrete Heating, *Int. J. Therm. Sci.*, 111 (2017), Jan., pp. 188-203
- [17] Gharbi, S., et al., Experimental Comparison between Different Configurations of PCM-Based Heat Sinks for Cooling Electronic Components, *Applied Thermal Engineering*, 87 (2015), Aug., pp. 454-462
- [18] Alshaer, W. G., et al., Thermal Management of Electronic Devices Using Carbon Foam and PCM/Nano-Composite, *International Journal of Thermal Sciences*, 89 (2015), Mar., pp. 79-86
- [19] Li, W. Q., et al., Enhanced Thermal Management with Microencapsulated Phase Change Material Particles Infiltrated in Cellular Metal Foam, *Energy*, 127 (2017), May, pp. 671-679
- [20] Zheng, H., et al., Thermal Performance of Copper Foam/Paraffin Composite Phase Change Material, *Energy Convers Manage*, 157 (2018), Feb., pp. 372-381
- [21] Huang, M. J., et al., Natural Convection in an Internally Finned Phase Change Material Heat Sink for the Thermal Management of Photovoltaics, *Solar Energy Materials & Solar Cells*, 95 (2011), 7, pp. 1598-1603
- [22] Vasu, A., et al., Corrosion Effect of Phase Change Materials in Solar Thermal Energy Storage Application, *Renew. Sustain. Energy Rev.*, 76 (2017), Sept., pp. 19-33
- [23] \*\*\*, [www.vedafrance.com](http://www.vedafrance.com)
- [24] Brent, A. D., et al., Enthalpy-Porosity Technique for Modeling Convection-Diffusion Phase Change: Application to the Melting of a Pure Metal, *Numer. Heat Transfer*, 13 (1988), 3, pp. 297-318
- [25] Ogoh, W., Groulx, D., Stefan's Problem: Validation of a One-Dimensional Solid-Liquid Phase Change Heat Transfer Process, *Proceedings, COMSOL Conference*, Boston, Mass., USA, 2010
- [26] \*\*\*, Heat Transfer Module, COMSOL MULTIPHYSICS, 2008